Trabecular bone structural variation throughout the human lower limb

Jaap P.P. Saers[a, *], Yasmin Cazorla Bak[a], Colin N. Shaw [a], Jay T. Stock[a], Timothy M. Ryan[b, c]

[a]PAVE Research Group, Department of Archaeology and Anthropology, Division of Biological Anthropology, University of Cambridge, Pembroke Street, Cambridge, United Kingdom

[b]Department of Anthropology, Pennsylvania State University, State College PA, 322 Carpenter Building, United States of America

[c]Center for Quantitative Imaging, EMS Energy Institute, Pennsylvania State University, State College PA, University Park, PA 16802, United States of America

*Corresponding author:

E-mail address: jpps2@cam.ac.uk (J.P.P. Saers)

Keywords: Functional morphology, Plasticity, Canalization, Mobility, Bone functional adaptation

Abstract

Trabecular bone is responsive to mechanical loading, and thus may be a useful tool for interpreting past behaviour from fossil morphology. However, the ability to meaningfully interpret variation in archaeological and hominin trabecular morphology depends on the extent to which trabecular bone properties are integrated throughout the postcranium or are locally variable in response to joint specific loading. We investigate both of these factors by comparing trabecular bone throughout the lower limb between a group of highly mobile foragers and two groups of sedentary agriculturalists. Trabecular bone structure is quantified in four volumes of interest placed within the proximal and distal joints of the femur and tibia. We determine how trabecular structures correspond to inferred behavioural differences between populations and whether the patterns are consistent throughout the limb. A significant correlation was found between inferred mobility level and trabecular bone structure in all volumes of interest along the lower limb. The greater terrestrial mobility of foragers is associated with higher bone volume fraction, and thicker and fewer trabeculae (lower connectivity density). In all populations, bone volume fraction decreases while anisotropy increases proximodistally throughout the lower limb. This observation mirrors reductions in cortical bone mass resulting from proximodistal limb tapering. The reduction in strength associated with reduced bone volume fraction may be compensated for by the increased anisotropy in the distal tibia. A similar pattern of trabecular structure is found throughout the lower limb in all populations, upon which a signal of terrestrial mobility appears to be superimposed. These results support the validity of using lower limb trabecular bone microstructure to reconstruct terrestrial mobility levels from the archaeological and fossil records. The results further indicate that care should be taken to appreciate variation resulting from differences in habitual activity when inferring behaviour from the trabecular structure of hominin fossils through comparisons with modern humans.

Introduction

Variation in cortical bone morphology has been used successfully to infer past behaviour in archaeological populations and hominin fossils (Ruff and Hayes, 1983; Stock and Pfeiffer, 2001; Holt, 2003; Marchi, 2008; Ruff, 2008; Shaw and Stock, 2009b; Stock et al., 2011; Macintosh et al., 2014; Ruff et al., 2015). Trabecular bone is also responsive to mechanical loading (Wolff, 1867; Huiskes et al., 2000; Pontzer et al., 2006; Sugiyama et al., 2010; Barak et al., 2011; Ryan and Shaw, 2015). While trabecular bone has been of interest for a long time (Macchiarelli et al., 1999), the increased availability of high resolution μCT scanning and high-throughput computing has made broad and detailed comparisons of primates and fossil hominins feasible (DeSilva and Devlin, 2012; Barak et al., 2013; Su et al., 2013; Skinner et al., 2015). Correlations between primate locomotor mode and trabecular microstructure have received much attention over the past decade and a half (Fajardo et al., 2002; Maga et al., 2006; Griffin et al., 2010; Lazenby et al., 2011; Ryan and Shaw, 2012; Scherf et al., 2013). However, variation in trabecular structure within and between modern human populations has not been considered widely in anthropology (Ryan and Shaw, 2015). The ability to infer behaviour from hominin fossils would be strengthened by a greater knowledge of adaptive constraints on morphology and clear evidence for a relationship between trabecular structural variation and inferred patterns of habitual activity in archaeological populations.

Bone tissue is well known to repair microdamage and model in response to mechanical loading (Frost, 2003). Bone is added under high dynamic strain (Sugiyama et al., 2010) and removed when dynamic strain is low (Squire et al., 2008). As a result, bone structure should reflect an individual's mechanical homeostasis. While long bone diaphyses are plastic in response to mechanical loading, the external morphology of joints is highly canalised (Rafferty and Ruff, 1994; Barak et al., 2011). In contrast, trabecular bone has been shown to be highly plastic in response to loading history (Pontzer et al., 2006; Barak et al., 2011; Wallace et al., 2013). While bone turnover rates vary substantially between anatomical locations and bone types, trabecular bone turnover is generally higher than that of cortical bone (Eriksen, 1986; Parfitt, 2002). Due to its complex structure, large

surface area, and high modeling rate, trabecular bone may be highly dynamic in its response to mechanical loading.

A considerable body of literature has now investigated trabecular bone variation across taxa in relation to primate locomotor patterns (Ryan and Ketcham, 2002; Fajardo et al., 2007; Griffin et al., 2010; Saparin et al., 2011; Ryan and Shaw, 2012; Shaw and Ryan, 2012) and allometric scaling (Doube et al., 2011; Barak et al., 2013; Fajardo et al., 2013; Ryan and Shaw, 2013). Experimental work on sheep (Barak et al., 2011), mice (Sugiyama et al., 2010; Wallace et al., 2013), and guinea fowl (Pontzer et al., 2006) has demonstrated the adaptability of trabecular bone in response to magnitude and directionality of mechanical loading, although in another study trabecular bone was not responsive to exercise induced loading (Wallace et al., 2012). A small number of studies have explored trabecular bone structure in hominin fossils (Macchiarelli et al., 1999; DeSilva and Devlin, 2012; Barak et al., 2013; Su et al., 2013; Skinner et al., 2015). While many aspects of external skeletal morphology may be constrained by phylogeny or function, the sensitivity of trabecular bone to mechanical loading in combination with high modeling rates may provide a dynamic source of data, reflecting the mechanical forces placed upon bones during life.

Before trabecular bone can be employed to infer past behaviour confidently from hominin fossils, we require a more nuanced understanding of the developmental, mechanical, and other physiological influences that underlie within-species variation in trabecular bone morphology. In comparison to interspecific research among other primates, trabecular bone variation within modern humans has not been thoroughly explored. Several studies have investigated the ontogeny of human trabecular bone across several anatomical locations (Ryan and Krovitz, 2006; Gosman and Ketcham, 2009; Raichlen et al., 2015). Raichlen et al. (2015) reported evidence that instability during the early stages of gait maturation is reflected in the trabecular structures of developing children. Ryan and Shaw (2015) demonstrated that modern human trabecular bone gracilisation in the proximal femur occurred after the shift from hunting and gathering to agriculture, which was associated with a general pattern of decreasing terrestrial mobility (Ruff et al., 1984, 2015; Macintosh et al., 2014). Ryan and Shaw (2015) found that hunter-gatherers displayed levels of trabecular bone volume fraction (BV/TV)

predicted for a primate of human body size. Less mobile agriculturalists were found to have significantly lower BV/TV for primates of their body size. These results demonstrate that modern humans are not systemically or uniformly gracile in trabecular bone structure. This suggests that human locomotor anatomy evolved in a physiological and mechanical context of high levels of loading throughout life (Ryan and Shaw, 2015). These results stress the need for the appreciation of human variation when performing comparative analyses between fossil hominins and modern humans or other primates.

Our ability to meaningfully interpret variation in trabecular bone structure depends largely on three issues—the response of bone tissue to mechanical loading, the extent to which trabecular bone properties are integrated throughout the postcranium, and the contribution of genes and developmental factors to the formation of trabecular bone structures. Theoretical and experimental work have demonstrated that not all regions of limb bone diaphyses are equally plastic in response to mechanical loading (Hallgrímsson et al., 2002; Skedros et al., 2003; Stock, 2006). There is an energetic trade-off between bone strength and mass, the effect of which becomes more pronounced distally along the lower limb. Bones must be strong enough to resist fracture but also as light as possible to reduce the energetic requirements of movement (Stock, 2006). Selective pressure for tissue economy appears to act less on proximal elements (Stock, 2006). Lower distal limb bone mass keeps the mass of the limb bones closer to the axis of rotation, which reduces the moment of inertia. This pattern is supported by evidence from the increasing frequency of fractures moving from proximal to more distal locations along the limbs of race-horses (Vaughan and Mason, 1975). Theory predicts a decrease in robusticity along individual limb bones, as well as along the limb as a whole, combined with reduced variability in strength in the more canalised distal elements (Pearson and Lieberman, 2004; Shaw et al., 2014). A pattern of decreasing proximo-distal robusticity is found in the diaphyseal strength of the human femur and tibia (Stock, 2006; Trinkaus and Ruff, 2012; Shaw et al., 2014). However, the predicted reduction in variation in the distal tibia has not been observed in the cortical morphology of the lower limb (Shaw et al., 2014). Recent work using pQCT scanning showed a decrease in trabecular bone mineral density throughout the lower limbs of cursorial and non-cursorial mammals, including

humans (Chirchir, 2015). However, the integration of trabecular bone morphology throughout the postcranium is poorly understood. The interplay between adaptation to local loading environment and potential morphological constraints on trabecular structure has not been explored.

In this paper, we will assess variation in trabecular microstructure throughout the lower limb within three archaeological populations. Our sample consists of one population of highly mobile hunter-gatherers and two more sedentary agriculturalist populations. First, we test the hypothesis that trabecular structure in the joints along the lower limb reflects inferred variation in mobility between the different populations. Second, we ask how trabecular structures are organised in the joints of the proximal and distal femur and tibia. We will test the hypothesis that, like cortical bone, trabecular bone will display a pattern of variation within the limb reflective of limb tapering. Finally, we will describe the patterns of variation in trabecular bone properties throughout the lower limbs to assess whether the joint specific loading environment in the lower limb is reflected in trabecular structure.

Materials and methods

Samples

Three populations with different levels of inferred mobility were used in this study (Table 1). Mobility is defined here as the total sum of all locomotor activities using the lower limb (Pearson et al., 2014). The hunter-gatherer population from Black Earth in southern Illinois is dated to 3000 B.C. and the site has been interpreted as a multi-season forager base camp (Jefferies and Avery, 1982; Jefferies, 2013). Individuals from the Black Earth site subsisted mainly on white-tailed deer, a wide range of other fauna, nuts, and seeds (Lopinot and Lynch, 1979, Brietburg, 1980). The Norris Farms #36 site is located in central Illinois, US, and associated with the Oneota culture. Dated to approximately 1300 A.D., the people from Norris Farms #36 practised a form of village agriculture supplemented with foraging. Their diet included deer, bison, fish, nuts, wild rice, corn, beans, and squash (Birmingham and Eisenberg, 2000). The Kerma derive from the ancient Nubian city of Kerma, one of the first urban centres that arose in eastern Africa. Kerma society was highly stratified, evidenced by large variation in the size of tombs and grave goods (Thompson et al., 2008). The

samples analysed represent a 12th Dynasty Nubian population of Nilotic intensive farmers, dated between 2100 and 1500 B.C. Comparisons of Kerma to other regional samples (Starling and Stock, 2007) indicate that they were in comparatively good health. Increased stature has also been observed in the Kerma population relative to earlier samples (Stock et al., 2011). Finally, the relatively low femoral midshaft robusticity of the Kerma population compared to earlier populations in the Nile Valley has been interpreted as evidence of reduced mobility associated with an agricultural lifestyle (Stock et al., 2011).

The three populations used in this study represent a gradient of mobility from highly terrestrially mobile (Black Earth) to highly sedentary (Kerma), with the Norris Farms #36 village agriculturalists intermediate between these two groups. Only non-pathological adult specimens were included in the current study. Trabecular bone can be significantly affected by age-related bone loss. Individuals showing osteological signs of old age were not included in the sample to limit possible effects of age-related bone loss. Age-at-death estimates for the Norris Farms and Black Earth populations were taken from existing museum collection records. Age-at-death for the Black Earth individuals was estimated using the multifactorial method described in Lovejoy et al. (1985), and transition analysis was used to estimate age-at-death for the Norris Farms (Milner and Smith, 1990). The mean ages in years for the Black Earth sample were 31.3 ± 4.39 for the males and 35 ± 9.51 for the females. The median ages (non-normal distribution) for the Norris Farms sample were 31.36 ± 4.39 for males and 26.9 ± 6.95 for the females. While no numerical estimates were given in museum records for the Kerma sample, only individuals aged as young and middle adult based on Buikstra and Ubelaker's (1994) standards were selected.

Computed tomography scanning and trabecular bone analysis

The proximal and distal aspects of the femur and tibia of the Norris Farms and Black Earth populations were scanned on the ONMI-X HD600 High-Resolution X-ray computed tomography (HRCT) scanner at the Center for Quantitative Imaging (CQI), Pennsylvania State University (Ryan and Krovitz, 2006; Shaw and Ryan, 2012; Macintosh et al., 2013; Ryan and Shaw, 2015). The Kerma

specimens were scanned using an identical protocol with a Nikon XTH 225 ST HRCT laboratory scanning system at the Cambridge Biotomography Centre, University of Cambridge. The Kerma HRCT scans were made using optimised energy settings (125 kV, 135 µA, 1080 views), and the Norris Farms and Black Earth scans were made using source energy settings 180 kV, 110 µA, and between 2800 and 4800 views. For the Norris Farms and Black Earth samples, resolution was maximised for the given size of the specimen resulting in resolutions between 0.050 and 0.057 mm. For the Kerma, the resolution was kept constant per anatomical location with 0.038 in the proximal femur, 0.048 in the distal femur, 0.042 in the proximal tibia, and 0.032 in the distal tibia.

Cubic volumes of interest were collected from the femoral head, the posterior half of the medial condyle of the distal femur, the medial condyle of the proximal tibia, and the distal tibia just beneath the talar articular surface using Avizo Fire 6.3 (Fig. 1). Kivell et al. (2011) have stressed the importance of VOI size and location and their effects on trabecular properties (Harrigan et al., 1988; Kivell et al., 2011). We placed the largest VOI possible in each joint in order to ensure that each VOI is reflective of structural variation between joints. The protocol ensured the VOI of each distal or proximal aspect was homologous in both location and size.

Once created, the cubic VOI was saved as a stack of dicom files and imported into ImageJ (http://rsbweb.nih.gov/ij/) to calculate the trabecular properties. Six trabecular bone morphometric variables were quantified using the BoneJ plugin (Doube, 2010). Bone volume fraction (BV/TV) is the volume of mineralised bone per unit volume. Trabecular thickness (Tb.Th) and trabecular separation (Tb.Sp) are calculated using model-independent distance transform methods (Hildebrand and Ruegsegger, 1997; Dougherty and Kunzelmann, 2007). Connectivity density (Conn.D) was calculated following the topological approach of Odgaard and Gundersen (1993). Degree of anisotropy (DA) was determined using the mean intercept length (MIL) method (Odgaard, 1997), calculated using a spherical volume centred in the cubic VOI to avoid edge and corner effects (Ketcham and Ryan, 2004). Bone surface-area-to-volume ratio (BS/BV) was calculated by dividing the total surface area of the three-dimensional triangulated surface by the calculated volume of the three-dimensional surface. Recent work has demonstrated that the widely used structure model index

is unsuitable for use on real bone geometries and was thus excluded from the analysis (Salmon et al., 2015).

Statistical analysis

Body mass (kg) estimates were calculated from measures of femoral head diameter (FHD). FHD was measured to 0.01 mm using Mitutoyo digital callipers. Estimates of body mass were calculated using the equations provided in Ruff et al. (1997). To assess the effect of variation in body mass on trabecular architecture in our sample, Ordinary Least Squares regressions were performed between structural variables and body mass. No relationships were found when comparing non-transformed and $\log_{10}$ transformed variables to non-transformed and $\log_{10}$ transformed body mass. Thus, standardisation for body mass was deemed unnecessary. Kruskal-Wallis and post hoc tests were performed in R version 3.2.0 by running a multiple comparison test after Kruskal-Wallis. To test for possible constraints on trabecular structural variation along the limb, we calculated the coefficients of variation for all properties within populations and in a pooled sample.

Results

The means and standard deviations of trabecular microstructural properties for the pooled sample and individual populations are listed in Table 2. First the differences in trabecular structure between populations will be described for each anatomical location. This is followed by a description of microstructural variation at each anatomical location throughout the lower limb in a pooled sample composed of all three populations.

Structural variation between populations

The results of the Kruskal-Wallis and post hoc tests of trabecular bone microstructural properties between populations are presented in Table 3 and are plotted in Figure 2. The Black Earth sample has significantly higher BV/TV compared to the other two populations in the proximal femur, and to the Kerma in all other VOIs as well. The Black Earth individuals have significantly lower Conn.D and BS/BV compared to the other two other populations in all VOIs. The Black Earth have

significantly thicker trabeculae compared to the Kerma in all locations, and compared to the Norris Farms in the proximal femur and proximal tibia. The Black Earth have significantly less anisotropic trabeculae in the distal tibia compared to the other populations.

The Norris Farms individuals have significantly lower BV/TV and Tb.Th than the Black Earth in the proximal femur, and significantly higher values compared to the Kerma in all VOIs. The Norris Farms individuals also have significantly higher DA in the femoral VOIs relative to the other populations, and significantly higher DA compared to the Black Earth in the distal tibia. The Norris Farms fall significantly below the Kerma in ConnD in all VOIs. BS/BV is significantly lower compared to the Kerma in the proximal femur and both tibial VOIs, but significantly higher than the Black Earth in the proximal femur.

The Kerma have significantly lower BV/TV, Tb.Th, and higher ConnD than the other populations. The Kerma have significantly lower femoral DA compared to the Norris Farms in both femoral VOIs, and significantly higher DA in the distal tibia compared to the Black Earth. Finally, they have significantly higher BS/BV than the other two populations, except in the distal femur.

Comparisons between joints in a pooled sample

The results of the Kruskal-Wallis and post hoc tests of trabecular properties between volumes of interest in a pooled sample are presented in Table 4 and Figure 2. No significant differences were found in Tb.Th or BS/BV along the lower limb in the pooled sample. The proximal femur has significantly higher BV/TV than the other VOIs. Trabeculae in the proximal femur are packed significantly closer together compared to the distal femur and tibia. The DA in the proximal femur is similar to that observed in the distal femur, but significantly more isotropic than in the proximal and distal tibia. The Conn.D results indicate that trabecular structure of the proximal femur is significantly more interconnected than that of the distal tibia, representing a higher number of trabeculae in the femoral head.

The distal femur has relatively low BV/TV, with thin and widely separated struts. Distal femoral trabecular structure is significantly less anisotropic than the tibial VOIs. Trabeculae in the distal femur are significantly more widely spaced apart than those in the proximal femur and tibia.

The trabecular structure of the proximal tibia is highly anisotropic with a low number of interconnected struts. The proximal tibia has significantly lower BV/TV than the proximal femur. It has significantly less trabecular spacing than the distal femur and distal tibia. Trabeculae are significantly more anisotropic than those found in the proximal and distal femur.

The distal tibia is characterised by a combination of the lowest BV/TV and the highest DA. Trabecular bone in the distal tibia is significantly more anisotropic compared to that of the proximal tibia and femur. Coefficients of variation did not display any distinctive patterns and did not decrease along the lower limb within populations or in the pooled sample (see Table 5).

Discussion

Are inferred levels of terrestrial mobility reflected in trabecular structure?

Our results indicate that human populations with divergent terrestrial mobility patterns display significantly different trabecular bone structure along the lower limb. The highly mobile foragers in our sample possess significantly more robust trabecular bone than both of the more sedentary agricultural groups. The mobile foragers have higher bone volume fraction, and fewer and relatively thick trabeculae, leading to low bone surface area to volume ratio. This pattern is especially evident in the proximal femur. Within the agricultural groups, the Norris Farms are significantly more robust than the Kerma in the proximal femur. While the Kerma were fully committed to agriculture, the Oneota people from the Norris Farms #36 site practised a mix of agriculture and foraging (Buikstra and Milner, 1991), and were thus expected to be more mobile than the Kerma but less mobile than the Black Earth. The distinctive pattern of fewer and thicker trabeculae with increasing levels of terrestrial mobility in Black Earth foragers may represent a relatively straightforward pattern

of skeletal responses to differing levels of mechanical loading in the human lower limb. These results suggest a relatively straightforward pattern of skeletal responses to differing levels of mechanical loading in the human lower limb.

The differences in individual structural properties between the three groups are pronounced in the proximal femur, but become less distinct moving distally along the lower limb. While the significant differences between the Kerma and the two more mobile populations persist throughout the lower limb, the differences between the Black Earth and the Norris Farms become less pronounced. Our results indicate significant variation in structure along the lower limb, suggesting that not all lower limb locations are equally sensitive to mechanical loading associated with mobility.

Trabecular bone structural features are highly correlated with the elastic properties of bone. High BV/TV, Tb.Th, and low Conn.D and BS/BV are associated with high levels of mechanical strain (Hodgskinson and Currey, 1990; Goulet et al., 1994; Odgaard et al., 1997; Kabel et al., 1999; Ulrich et al., 1999; Rubin et al., 2002; Mittra et al., 2005; Rincón-Kohli and Zysset, 2009; Barak et al., 2011; Karim and Vashishth, 2011; Ryan and Shaw, 2015). Bone volume fraction is a common predictor of fracture risk in clinical settings and correlates strongly with ultimate bone strength and elastic modulus (Ulrich et al., 1999; Mittra et al., 2005). In addition to BV/TV, trabecular structural organization (Tb.Th, Tb.Sp, Conn.D, DA) has been shown to play a significant role in bone's resistance to fracture. Trabecular thickness correlates positively with elastic modulus and ultimate strength (Rubin et al., 2002; Mittra et al., 2005). The fabric anisotropy is also of significant importance to the stiffness of trabecular structures (Odgaard et al., 1997; Ulrich et al., 1999), and has been found to correlate significantly to ultimate strength and elastic modulus (Mittra et al., 2005). Trabecular bone is stiffest when loaded in the primary direction in which struts are oriented (Odgaard et al., 1997). These relationships between elastic properties and trabecular bone structure, independent of the constitutive material properties, provides an opportunity to use trabecular bone structural variation as a tool to interpret behavioural patterns in past human groups. Our results support the hypothesis that trabecular bone properties are reflective of mechanical loading history in these human groups with divergent behavioural patterns and, therefore, can potentially be used to evaluate and

reconstruct patterns and levels of terrestrial mobility in the past. Future work should investigate whether the mobility signals observed between these populations hold up in a wider range of archaeological populations, and whether subtle differences in activity between largely mobile Palaeolithic populations can be detected. This could be tested experimentally using animal models, but advances to high resolution pQCT now allows researchers to also study living humans. The effects of large as well as subtle variation in behaviour can be tested using modern human athletes participating at different levels in various sports. While we have demonstrated a link between terrestrial mobility and lower limb trabecular bone variation, the next logical step is to also investigate the upper limbs of different human populations with different inferred manual activity regimes. The first question that needs to be answered conclusively is whether trabecular bone adapts locally or systemically to levels of physical activity. Variation in upper limb diaphyseal cross-sectional geometry is indicative of habitual upper limb loading and has been used to interpret behaviour in archaeological populations (Trinkaus et al., 1994; Stock and Pfeiffer, 2001; Shaw and Stock, 2009a). Previous work indicates that the relationship between trabecular structure and diaphyseal cross-sectional geometry is not always straightforward (Shaw and Ryan, 2012). Shaw and Ryan (2012) found correlations between humeral head trabecular structure and mid-humerus diaphyseal bone properties, but found none in the femur. In interspecific comparisons between femoral and humeral diaphyseal cross-sectional geometry, Shaw and Ryan (2012) found an osteological locomotor signal, but not in trabecular bone architecture. However, in a subsequent paper using discriminant function analysis of trabecular bone properties in the femoral head and humeral head, distinct trabecular locomotor signatures were found between primate locomotor modes (Ryan and Shaw, 2012). Using principal components analysis, Scherf et al. (2013) also managed to clearly distinguish between the proximal humeral trabecular structure of humans, chimpanzees, and orangutans. Scherf et al. (2016) compared humeral head trabecular bone properties of Neolithic and contemporary human samples. The Neolithic population was predicted to have a higher physical workload compared to contemporary humans. They found significantly higher values of humeral BV/TV in a Neolithic human population compared to a modern contemporary sample. The work of Shaw and Ryan (2012), Ryan and Shaw (2012, 2015), Scherf et al. (2013, 2016), and the current study indicates that while the

relationship between trabecular structure and diaphyseal cross-sectional geometry is not always straightforward, both appear to be informative of loading history.

Despite the recognition of a locomotor behavioural signal, there are several limitations to the conclusions we can draw from this data, the most prominent of which is the sample diversity. Three archaeological populations were compared with approximate mobility levels ranked relative to each other. The Kerma group is derived from a geographically and climatically different environment, with more significant genetic differences to the North American groups due to their Northeast African ancestry, factors that may have contributed to the observed differences (Turner et al., 2000; Stock, 2006; Wallace et al., 2012). However, the Black Earth and Norris Farms collections derive from geographically and climatically proximate sites in Illinois, USA, with differences less likely to be explained by ancestry. The influence of sex was compensated for by selecting roughly equal numbers of males and females from each population. The largest discrepancy in the ratio of males to females is found in the Kerma population (M = 13, F = 7). Independent *t*-tests were used to assess possible sex differences within the three populations and a pooled sample but no significant differences were found in the trabecular properties in any population. Another factor known to influence bone biology is diet. The dietary shift towards cultivated grains in agriculturalists is associated with reduced calcium intake in some populations (Eaton and Nelson, 1991; Heaney, 2003). The archaeological record provides some insight into the diets of the three populations. Stable isotope, archaeobotanical, and zoological data point towards a broad diet consumed by the inhabitants of Kerma. The faunal dietary component consisted of a mix of sheep, goat, cattle, and aquatic resources. Cereals were excavated from bakeries that housed rows of ovens capable of producing large quantities of bread (Bonnet, 1988). The cemetery also yielded grains of barley (*Hordeum vulgare*), cucurbits (Curcurbitaceae), and legumes (Leguminosae) (Thompson et al., 2008). The Norris Farms engaged in a mixed subsistence strategy that combined the cultivation of maize and other plants with hunting, fishing, and gathering of wild plants (Buikstra and Milner, 1991). The Black Earth foragers subsisted on a diverse diet of large and small mammals, birds, fish, and seasonally available plant resources (Jefferies and Lynch, 1983). In addition to the mobility differences, these dietary factors could have

contributed to a reduction in bone mass in the agriculturalists compared to foragers. Finally, the relative contributions of the mechanical and genetic environment to trabecular bone ontogeny are poorly understood and require further investigation (Judex et al., 2004; Wallace et al., 2012). Despite the effects of confounding variables, past work suggests activity plays a significant role in determining skeletal strength and robusticity (Ruff et al., 1984; Bridges, 1989; Stock and Pfeiffer, 2001; Shaw and Stock, 2009b, 2013; Ryan and Shaw, 2015).

Microstructural variation Throughout the lower limb

While the three populations showed significant differences in the trabecular bone structural properties throughout the lower limb, some distinct patterns can be observed. All groups displayed a similar trend of proximodistal reductions in BV/TV along the femur and tibia, and along the lower limb as a whole. Additionally, in all populations the femoral VOIs were significantly more isotropic than the tibia. Trabecular bone in the three populations follows the same design constraints as cortical bone: significant structural tapering exists within the femur and tibia, as well as along the lower limb as a whole (Stock, 2006; Shaw et al., 2014; Chirchir, 2015). The proximal femur is characterised by having the highest BV/TV and the highest number of struts. The distal tibia has the lowest BV/TV combined with the most anisotropic structure. The variables at the knee joint are generally intermediate between those of the hip and ankle. No significant differences in Tb.Th were found throughout the lower limb in the pooled sample, and within populations only in the Kerma, where the proximal femur had thicker trabeculae than the distal tibia. Thus, the decrease in BV/TV found along the lower limb does not appear to be driven by a decrease in strut thickness. The increase in Tb.Sp and decrease in BV/TV, combined with the equal amount of Tb.Th found in the distal femur and tibia, suggests that a decrease in the number of trabeculae may be driving the gracilisation along the lower limb. Lower limb tapering keeps the mass of the limb bones closer to the axis of rotation, which reduces the moment of inertia. It has been proposed that one of the factors controlling the tapering of robusticity along the lower limb is a greater level of canalisation in the distal limb segments (Hallgrímsson et al., 2002; Stock, 2006). If trabecular structure is proximodistally canalised, one

would predict lower levels of inherent variation within individual and pooled populations in distal segments (Shaw et al., 2014). Shaw et al. (2014) did not find a reduction in coefficients of variation of cortical bone throughout the lower limbs. Similarly, in the current study, CVs for trabecular bone did not decrease along the lower limb within populations or in the pooled sample. Unlike the clear pattern of decreasing trabecular BV/TV along the lower limb, a corresponding trend of decreasing structural variability is not found (see Table 5).

If trabecular bone mass is constrained distally, then other macro- or microstructural adaptations may be favoured over adaptations that increase relative bone volume. The increased anisotropy in the tibia may reduce the requirement of additional bone mass by aligning the trabecular structure in the primary direction of loading. More likely, however, higher anisotropy may be reflective of the more constrained, unidirectionally loaded joints of the proximal and distal tibia. These differences in fabric anisotropy may also reflect differences in bone shape between the relatively straight tibia and the more complexly shaped femur. Raichlen et al. (2015) found an increase in DA and a decrease in variability in DA between individuals associated with increasing balance and neuromuscular control during locomotor development in human children. Barak et al. (2013) found significantly more isotropic trabecular bone in the distal tibia of chimpanzees compared to modern humans and *Australopithecus africanus*. This finding was interpreted as the result of a greater range of loading orientations during climbing and other activities in chimpanzees (Barak et al., 2013). In the current study, we found substantially less variation in the DA in the distal tibia compared to the femur in all populations (Table 5), indicating that this may indeed may be a distinctive feature of adult human bipedal locomotion. While the *Au. africanus* specimen with the highest BV/TV included in the study by Barak et al. (2013) had considerably higher BV/TV than their most robust human specimen, it falls within one standard deviation of the Black Earth mean BV/TV and thus within the human range of variation. However, caution should be employed when comparing results from different studies, as variation in VOI size and location can significantly affect mean trabecular properties (Kivell et al., 2011). Ryan and Shaw (2012, 2015) investigated trabecular architecture in the femoral head of 32 primate species including humans and found that humans have

highly anisotropic structures compared to quadrupedal primates. This matches predictions of the stereotypical loading at the hip joint imposed during bipedal locomotion compared to quadrupedal and climbing apes, which are likely to experience more diverse postural and locomotor loads. These interspecific analyses combined with the results from the current study demonstrate the correspondence of trabecular bone structure to habitual loading and indicate that the analysis of trabecular bone variation may be a useful tool to interpret behaviour in the hominin fossil record. Postcranial morphology suggest that Australopithecine locomotor repertoires most likely included an arboreal component alongside terrestrial bipedalism, although retentions of primitive traits are difficult to dismiss (Ward, 2002). Based on the results of these interspecific analyses and the current study, Australopithecines would be expected have lower levels of DA compared to humans but higher DA compared to arboreal primates. Barak et al. (2013) did indeed find levels of DA in the distal tibia of *Australopithecus africanus* between those of humans and chimpanzees. In terms of future work in this direction, we suggest that a combined study of the upper limbs and feet alongside the lower limbs may present a more nuanced picture of the relationships between postcranial trabecular morphology and locomotor behaviour.

Several factors are potentially driving the observed similarities between the human populations in the patterns of trabecular bone structure throughout the lower limb. These include variation in joint specific loading conditions, variation in joint morphology along the limb, and canalisation of structure through growth and development. More data are needed to understand the differences in magnitude and direction of joint moments throughout the lower limb during normal bipedal locomotion. The contact forces at the hip, knee, and ankle have been measured with implants instrumented with strain gauges (Bergmann et al., 2001; Heller et al., 2001; Stansfield et al., 2003; Foucher et al., 2012). Peak contact force at the hip joint during normal walking has been measured between 2.5 and 4.6 times body weight, and 5.5 times body weight during jogging (Bergmann et al., 1993, 2001). Peak contact forces at the knee have been measured in vivo at 2.1–2.9 times body weight (Taylor et al., 2004). The medial side of the knee experiences significantly greater loads compared to the lateral side. The reaction forces on the ankle joint are equal to or greater than those on the hip and

knee (Hagins and Pappas, 2012). Maximum compressive ankle joint reaction force was 4.6 times body weight (Stauffer et al., 1977). During weight bearing, 77–90% of the load is transmitted through the tibial plafond to the talar dome depending on foot position (Calhoun et al., 1994). It should be noted that these are just normal walking forces. Activities such as running, standing from a sitting position, or climbing stairs can produce forces much higher on different joints. The greater BV/TV of the femoral head may result from the fact that, unlike the other joints, the femoral head is continuously loaded during daily activities. However, joint contact forces alone do not explain the pattern of trabecular bone volume fraction along the lower limb. Trabecular structure at the distal tibia has the lowest bone volume fraction despite being subjected to the highest peak loading. The high degree of anisotropy in the distal tibia likely compensates for the low bone mass by aligning into the primary direction of loading. The combination of low BV/TV and high anisotropy in the distal tibia may be explained by the canalisation of bone mass in the distal limb, combined with structural optimisation for strength relative to habitual loading, however, it leaves the distal tibia more vulnerable to fractures resulting from eccentric loading.

Variation in joint function and joint morphology likely influences underlying trabecular bone structure (Patel and Carlson, 2007). The femoral head is a highly mobile ball and socket joint, whereas the knee and ankle are hinge joints with more restricted movement. While the direction of force transmitted through the tibial joints mostly travels in the same direction, the proximal and distal femur are exposed to more varied loading directions during gait (Frankel et al., 2012; Hagins and Pappas, 2012; Sheikzadeh et al., 2012). The greater range of joint loading directions of the proximal and distal femur joints accounts for the lower DA in the femur compared to the tibia. A final possibility is that the observed patterns are the result of developmental processes with proximal and distal epiphyses canalised into somewhat hardwired growth trajectories upon which loading related to mobility levels is superimposed. Further work on the development of trabecular structures during ontogeny in relation to gait maturation and growth are required to evaluate this possibility. It is expected that the tapered trabecular pattern observed in this study is not unique to humans among hominins. Chirchir (2015) used pQCT to investigate whether trabecular bone mass in the distal limbs

is relatively lower than that in the proximal limb in cursorial compared to non-cursorial species in hominids, cercopithecines, and felids. A proximodistal decrease in trabecular bone mass was observed irrespective of cursoriality in hominid and cercopithecine hind limbs, indicating that this tapered pattern is likely present in fossil hominins as well, and may not be a good indicator of cursoriality. It should be noted that Chirchir (2015) only investigated trabecular bone mass but not its morphology. While comparative data is not present, we suspect that cursors may be differentiated from non-cursors by increased DA, resulting from more uniform limb loading.

While all of the considerations discussed in this paper can account for some of the variation we observe in human lower limb trabecular microstructure, no single factor explains all observations. We have found patterns of decreasing trabecular bone volume fraction along the lower limb as well as in limb segments, in similar fashion to cortical bone strength along the lower limb bone shafts. The mobility gradients appear to be superimposed upon this pattern of proximodistal variation. The exact mechanism behind this observation requires further investigation.

Conclusions

To infer behaviour from hominin fossil morphology, a more thorough understanding of within species variation and adaptive constraints on trabecular structure is required. We have documented the variation in trabecular microstructural organisation along the lower limb between three human populations with different inferred terrestrial mobility patterns. Significant differences were found throughout the lower limb between the three populations, indicating that trabecular bone structure along the lower limb reflects terrestrial mobility levels. However, not all lower limb regions were equally sensitive to loading associated with the inferred levels of terrestrial mobility. Femoral head microstructure was found to most successfully separate the three populations based on variation in individual structural properties.

While the average magnitudes of structural properties differ significantly between populations, similar patterns in structural properties are observed along the lower limb. Trabecular

structures follow the same tapered design as cortical bone in the shafts of long bones. There are signals indicating that trabecular bone adapts to joint specific loading conditions, evidenced by the reduction in anisotropy in the femoral VOIs that is associated with a higher joint mobility compared to the tibia. However, the distal tibia had the lowest bone volume fraction despite experiencing the highest peak loading of all joints, arguing for a certain degree of morphological constraint. No significant differences in the coefficients of variation of trabecular properties were found throughout the limb. Thus, there may be a baseline pattern of trabecular bone variation throughout the lower limb upon which a mobility signal is imposed, but the mechanisms driving the observed patterns require further study. Comparisons of structural variation along the lower limb should be performed with a more diverse sample of human populations and nonhuman primates, in order to determine whether the patterns described in this study are unique to human bipedal locomotion. By carefully selecting human groups for comparison, a better understanding of the range of variation among human populations and the environmental and behavioural conditions under which trabecular bone structure varies can be obtained. Future work combining kinematic and kinetic studies with finite element modelling may be able to shed additional light on the mechanisms controlling human lower limb microstructure. The findings reported in this study are relevant to fields including human evolution, bone biology, reconstructions of past activity, and bone health in contemporary human populations.

We have demonstrated a strong relationship between terrestrial mobility and trabecular variation throughout the lower limb within human populations. A number of major shifts occurred in hominin evolution with the emergence of *Homo erectus* ~1.8 million years ago, including increased variation in body size (Will and Stock, 2015), increased brain size (McHenry and Coffing, 2000), greater efficiency of bipedal locomotion (Pontzer, 2007), and increased mobility (Braun et al., 2009). The long evolutionary history of high levels of physical activity in *Homo* suggests that the human skeleton evolved in a mechanical context involving high levels of persistent loading throughout life (Bramble and Lieberman, 2004; Raichlen et al., 2012; Shaw and Stock, 2013). Previous work on trabecular bone (Chirchir et al., 2015; Ryan and Shaw, 2015) and cortical bone (Holt, 2003; Shaw and Stock, 2013; Macintosh et al., 2014; Ruff et al., 2015) shows a substantial decrease in bone mass in

human populations associated with increased sedentism after the adoption of agriculture. Reduced physical activity is thought to be a major cause for the increased prevalence of osteoporosis in contemporary society (Borer, 2005). while we have demonstrated significant variation between populations with substantially different inferred mobility levels, it is not clear if trabecular bone can pick up subtler behavioural differences. It is thus unknown whether trabecular bone can be employed to investigate behaviour in pre-agricultural populations who are all thought to have been largely mobile.

There are important trends in robusticity throughout human evolution, particularly in the last 10,000 years. To confidently interpret these trends, we must gain a more detailed understanding of the factors that influence trabecular bone microstructure. There is significant potential for using trabecular structural variation to inform behavioural inferences from fossils. However, before hominin behaviour can be inferred, we require a greater appreciation of the possible variation in modern and past *Homo sapiens*. Previous work has tended to focus on one particular anatomical location, but this study has demonstrated the value of investigating patterns of trabecular microstructure throughout the lower limb. In order to investigate whether species specific patterns of trabecular bone structure can be distinguished, future research should focus on trabecular variation in multiple anatomical locations throughout the postcranium in multiple human populations and primate species, and consider multivariate analyses to complement univariate comparisons of trabecular properties. Advances in high resolution pQCT scanning now allows trabecular bone to be quantified in living humans, opening up the possibility of investigating trabecular structure in high level athletes. This type of work will result in a detailed framework in which fossil trabecular morphology can be confidently examined and interpreted in the context of locomotor behaviour and physical activity levels.

Acknowledgements

We thank Terrance Martin at the Illinois State Museum, George Milner at Pennsylvania State University, Heather Lapham at the Center for Archaeological Investigations, Southern Illinois

University Carbondale, and Marta Mirazón Lahr at the Leverhulme Centre for Human Evolutionary Studies, University of Cambridge, for providing access to skeletal material. The research leading to these results has received funding from the European Research Council under the European Union's Seventh Framework Programme (FP/2007-2013) / ERC Grant Agreement n.617627 (to JTS), the Arts and Humanities Research Council Doctoral Training Programme, AH/14/Archaeology/3 (to JPPS), and National Science Foundation Grant BCS-0617097 (to TMR). Finally, we thank editor Sarah Elton, an associate editor, and two anonymous reviewers whose efforts greatly improved this manuscript.

References

Barak, M., Lieberman, D., Hublin, J., 2013. Of mice, rats and men: Trabecular bone architecture in mammals scales to body mass with negative allometry. J. Struct. Biol. 183, 123–131.

Barak, M.M., Lieberman, D.E., Hublin, J.-J., 2011. A Wolff in sheep's clothing: trabecular bone adaptation in response to changes in joint loading orientation. Bone 49, 1141–51.

Barak, M.M., Lieberman, D.E., Raichlen, D., Pontzer, H., Warrener, A.G., Hublin, J.-J., 2013. Trabecular evidence for a human-Like gait in Australopithecus africanus. PLoS One 8, e77687.

Bergmann, G., Graichen, F., Rohlmann, A., 1993. Hip joint loading during walking and running, measured in two patients. J. Biomech. 26, 969–990.

Bergmann, G., Deuretzbacher, G., Heller, M., Graichen, F., Rohlmann, A., Strauss, J., Duda, G.N., 2001. Hip contact forces and gait patterns from routine activities. J. Biomech. 34, 859–871.

Borer, K.T., 2005. Physical activity in the prevention and amelioration of osteoporosis in women : interaction of mechanical, hormonal and dietary factors. Sports Med. 35, 779–830.

Bramble, D.M., Lieberman, D.E., 2004. Endurance running and the evolution of Homo. Nature 432, 345–52.

Braun, D.R., Harris, J.W.K., Maina, D.N., 2009. Oldowan raw material procurement and use: evidence from the Koobi Fora formation. Archaeometry 51, 26–42.

Bridges, P.S., 1989. Changes in Activities with the Shift to Agriculture in the Southeastern United States. Curr. Anthropol. 30, 385–394.

Buikstra, J.E., Milner, G.R., 1991. Isotopic and archaeological interpretations of diet in the central mississippi valley. J. Archaeol. Sci. 18, 319–329.

Calhoun, J.H., Li, F., Ledbetter, B.R., Viegas, S.F., 1994. A comprehensive study of pressure distribution in the ankle joint with inversion and eversion. Foot Ankle Int. 15, 125–133.

Chirchir, H., 2015. A comparative study of trabecular bone mass distribution in cursorial and Non-

cursorial limb joints. Anat. Rec. 298, 797–809.

Chirchir, H., Kivell, T.L., Ruff, C.B., Hublin, J., Carlson, K.J., Zipfel, B., 2015. Recent origin of low trabecular bone density in modern humans. Proc. Natl. Acad. Sci. 112, 366–371.

DeSilva, J.M., Devlin, M.J., 2012. A comparative study of the trabecular bony architecture of the talus in humans, non-human primates, and Australopithecus. J. Hum. Evol. 63, 536–51.

Doube, M., 2010. BoneJ: free and extensible bone image analysis in Image J. Bone 47, 1076 – 1079.

Doube, M., Klosowski, M.M., Wiktorowicz-Conroy, A.M., Hutchinson, J.R., Shefelbine, S.J., 2011. Trabecular bone scales allometrically in mammals and birds. Proc. Biol. Sci. 278, 3067–73.

Dougherty, R., Kunzelmann, K.-H., 2007. Computing local thickness of 3D structures with ImageJ. Microsc. Microanal. 13, 1678–1679.

Eaton, B., Nelson, D., 1991. Calcium in evolutionary perspective. Am. J. Clin. Nutr. 281 – 287.

Eriksen, E.F., 1986. Normal and pathological remodeling of human trabecular bone: three dimensional reconstruction of the remodeling sequence in normals and in metabolic bone disease. Endocr. Rev. 7, 379 – 408.

Fajardo, R.J., Ryan, T.M., Kappelman, J., 2002. Assessing the accuracy of high-resolution X-ray computed tomography of primate trabecular bone by comparisons with histological sections. Am. J. Phys. Anthropol. 118, 1–10.

Fajardo, R.J., Müller, R., Ketcham, R. A, Colbert, M., 2007. Nonhuman anthropoid primate femoral neck trabecular architecture and its relationship to locomotor mode. Anat. Rec. 290, 422–436.

Fajardo, R.J., Desilva, J.M., Manoharan, R.K., Schmitz, J.E., Maclatchy, L.M., Bouxsein, M.L., 2013. Lumbar vertebral body bone microstructural scaling in small to medium-sized strepsirhines. Anat. Rec. 296, 210–226.

Foucher, K., Wimmer, M., Andersson, G., 2012. Biomechanics of Arthroplasty. In: Nording, M., Frankel, V.H. (Eds.), Basic biomechanics of the musculoskeletal system. Wolters Kluwer ,Baltimore, pp. 404 – 425.

Frankel, V.H.., Nording, M.., Walker, P.S.., 2012. Biomechanics of the Knee. In: Nording, M., Frankel, V.H. (Eds.), Basic Biomechanics of the Musculoskeletal System. Wolters Kluwer ,Baltimore, pp. 280–205.

Frost, H.M., 2003. Bone's mechanostat: a 2003 update. Anat. Rec. A. Discov. Mol. Cell. Evol. Biol. 275, 1081–101.

Gosman, J.H., Ketcham, R.A., 2009. Patterns in ontogeny of human trabecular bone from SunWatch Village in the Prehistoric Ohio Valley: general features of microarchitectural change. Am. J. Phys. Anthropol. 138, 318–32.

Goulet, R.W., Goldstein, S.A, Ciarelli, M.J., Kuhn, J.L., Brown, M.B., Feldkamp, L.A, 1994. The relationship between the structural and orthogonal compressive properties of trabecular bone. J. Biomech. 27, 375–89.

Griffin, N.L., D'Août, K., Ryan, T.M., Richmond, B.G., Ketcham, R.A., Postnov, A., 2010. Comparative forefoot trabecular bone architecture in extant hominids. J. Hum. Evol. 59, 202–13.

Hagins, M., Pappas, E., 2012. Biomechanics of the Foot and Ankle. In: Nording, M., Frankel, V.H. (eds.), Basic biomechanics of the musculoskeletal system. Wolters Kluwer, Baltimore, pp. 224 – 253.

Hallgrímsson, B., Willmore, K., Hall, B.K., 2002. Canalization, developmental stability, and morphological integration in primate limbs. Yearb. Phys. Anthropol. 45, 131–158.

Harrigan, T., Jasty, M., Mann, R., Harris, W., 1988. Limitations of the continuum assumption in cancellous Bone. J. Biomech. 21, 269–275.

Heaney, R.P., 2003. Is the paradigm shifting? Bone 33, 457–465.

Heller, M.., Bergmann, G., Deuretzbacher, G., Dürselen, L., Pohl, M., Claes, L., Haas, N., Duda, G., 2001. Musculo-skeletal loading conditions at the hip during walking and stair climbing. J. Biomech. 34, 883–893.

Hildebrand, T., Ruegsegger, P., 1997. A new method for the model-independent assessment of

thickness in three-dimensional images. J. Microsc. 185, 67–75.

Hodgskinson, R., Currey, J.D., 1990. The effect of variation in structure on the young's modulus of cancellous bone: a comparison of human and non-human material. Proc. Inst. Mech. Eng. Part H J. Eng. Med. 204, 115 – 121.

Holt, B.M., 2003. Mobility in Upper Paleolithic and Mesolithic Europe: evidence from the lower limb. Am. J. Phys. Anthropol. 122, 200–15.

Huiskes, R., Ruimerman, R., van Lenthe, G.H., Janssen, J.D., 2000. Effects of mechanical forces on maintenance and adaptation of form in trabecular bone. Nature. 405, 704–6.

Jefferies, R.., Lynch, B.., 1983. Dimensions of Middle Archaic Cultural Adaptation at the Black Earth Site, Saline County, Illinois. Archaic Hunters Gatherers Am. Midwest. Academic Press, New York, pp. 299–322.

Jefferies, R.W., 2013. The Archaeology of Carrier Mills: 10,000 Years in the Saline Valley of Illinois. Carbondale. Southern Illinois University Press, Carbondale, pp. 1-186.

Jefferies, R.W., Avery, G.E., 1982. The Carrier Mills Archaeological Project: Human Adaptation in the Saline Valley. Southern Illinois University Press, Carbondale.

Judex, S., Garman, R., Squire, M., Donahue, L.-R., Rubin, C., 2004. Genetically based influences on the site-specific regulation of trabecular and cortical bone morphology. J. Bone Miner. Res. 19, 600–606.

Kabel, J., Odgaard, A, van Rietbergen, B., Huiskes, R., 1999. Connectivity and the elastic properties of cancellous bone. Bone 24, 115–20.

Karim, L., Vashishth, D., 2011. Role of trabecular microarchitecture in the formation, accumulation, and morphology of microdamage in human cancellous bone. J. Orthop. Res. 29, 1739–1744.

Ketcham, R.A, Ryan, T.M., 2004. Quantification and visualization of anisotropy in trabecular bone. J. Microsc. 213, 158–171.

Kivell, T.L., Skinner, M.M., Lazenby, R., Hublin, J.-J., 2011. Methodological considerations for

analyzing trabecular architecture: an example from the primate hand. J. Anat. 218, 209–25.

Lazenby, R.A, Skinner, M.M., Hublin, J.J., Boesch, C., 2011. Metacarpal trabecular architecture variation in the chimpanzee (*Pan troglodytes*): Evidence for locomotion and tool-use? Am. J. Phys. Anthropol. 144, 215–225.

Lovejoy, C.O., Meindl, R.S., Mensforth, R.P., Barton, T.J., 1985. Multifactorial determination of skeletal age at death: a method and blind tests of its accuracy. Am. J. Phys. Anthropol. 68, 1–14.

Macchiarelli, R., Bondioli, L., Galichon, V., Tobias, P.V, 1999. Hip bone trabecular architecture shows uniquely distinctive locomotor behaviour in South African australopithecines. J. Hum. Evol. 36, 211–32.

Macintosh, A.A., Davies, T.G., Ryan, T.M., Shaw, C.N., Stock, J.T., 2013. Periosteal versus true cross-sectional geometry: a comparison along humeral, femoral, and tibial diaphyses. Am. J. Phys. Anthropol. 150, 442–52.

Macintosh, A.A., Pinhasi, R., Stock, J.T., 2014. Lower limb skeletal biomechanics track long-term decline in mobility across ~6150 years of agriculture in Central Europe. J. Archaeol. Sci. 52, 376–390.

Maga, M., Kappelman, J., Ryan, T.M., Ketcham, R.A, 2006. Preliminary observations on the calcaneal trabecular microarchitecture of extant large-bodied hominoids. Am. J. Phys. Anthropol. 129, 410–7.

Marchi, D., 2008. Relationships between lower limb cross-sectional geometry and mobility: The case of a Neolithic sample from Italy. Am. J. Phys. Anthropol. 137, 188–200.

McHenry, H.M., Coffing, K., 2000. Australopithecus to Homo: Transformations in body and mind. Annu. Rev. Anthropol. 29, 125–146.

Milner, G.R., Smith, V.G., 1990. Oneata human skeletal remains. In: Santure, S., Harn, A., Esarey, D. (Eds.), Archaeological Investigations at the Morton Village and Norris Farms 36 Cemetery. Illinois State Museum, Springfield, pp. 111–148.

Mittra, E., Rubin, C., Qin, Y.X., 2005. Interrelationship of trabecular mechanical and microstructural properties in sheep trabecular bone. J. Biomech. 38, 1229–1237.

Odgaard, A., 1997. Three-dimensional methods for quantification of cancellous bone architecture. Bone 20, 315–328.

Odgaard, A., Gundersen, H.J., 1993. Quantification of connectivity in cancellous bone, with special emphasis on 3-D reconstructions. Bone 14, 173–82.

Odgaard, A., Kabel, J., van Rietbergen, B., Dalstra, M., Huiskes, R., 1997. Fabric and elastic principal directions of calcellous bone are closely related. J. Biomech. 30, 487 – 495.

Parfitt, A.M., 2002. Misconceptions (2): turnover is always higher in cancellous than in cortical bone. Bone 30, 807–809.

Patel, B.A., Carlson, K.J., 2007. Bone density spatial patterns in the distal radius reflect habitual hand postures adopted by quadrupedal primates. J. Hum. Evol. 52, 130–141.

Pearson, O.M., Lieberman, D.E., 2004. The aging of Wolff's "law": ontogeny and responses to mechanical loading in cortical bone. Am. J. Phys. Anthropol. Suppl 39, 63–99.

Pearson, O.M., Petersen, T., Sparacello, V.S., Daneshvari, S., Grine, F.E., 2014. Activity, "body shape", and cross-sectional geometry of the femur and tibia. In: Carlson, K.J., Marchi, D. (eds), Reconstructing mobility: environmental, behavioral, and morphological determinants. Springer, New York.

Pontzer, H., 2007. Effective limb length and the scaling of locomotor cost in terrestrial animals. J. Exp. Biol. 210, 1752–1761.

Pontzer, H., Lieberman, D.E., Momin, E., Devlin, M.J., Polk, J.D., Hallgrímsson, B., Cooper, D.M.L., 2006. Trabecular bone in the bird knee responds with high sensitivity to changes in load orientation. J. Exp. Biol. 209, 57–65.

Rafferty, K.L., Ruff, C.B., 1994. Articular structure and function in Hylobates, Colobus, and Papio. Am. J. Phys. Anthropol. 94, 395–408.

Raichlen, D.A., Foster, A.D., Gerdeman, G.L., Seillier, A., Giuffrida, A., 2012. Wired to run: exercise-induced endocannabinoid signaling in humans and cursorial mammals with implications for the “runner”s high’. J. Exp. Biol. 215, 1331–1336.

Raichlen, D.A., Gordon, A.D., Foster, A.D., Webber, J.T., Sukhdeo, S.M., Scott, R.S., Gosman, J.H., Ryan, T.M., 2015. An ontogenetic framework linking locomotion and trabecular bone architecture with applications for reconstructing hominin life history. J. Hum. Evol. 81, 1–12.

Rincón-Kohli, L., Zysset, P.K., 2009. Multi-axial mechanical properties of human trabecular bone. Biomech. Model. Mechanobiol. 8, 195–208.

Rubin, C., Turner, A.S., Müller, R., Mittra, E., McLeod, K., Lin, W., Qin, Y.-X., 2002. Quantity and quality of trabecular bone in the femur are enhanced by a strongly anabolic, noninvasive mechanical intervention. J. Bone Miner. Res. 17, 349–357.

Ruff, C.B., 2008. Biomechanical Analyses of Archaeological Human Skeletons. In: Katzenberg, M.A., Saunders, S.R., (eds.), Biological anthropology of the human skeleton. John Wiley & Sons, Inc., New Jersey, pp. 183 – 206.

Ruff, C.B., Hayes, W.C., 1983. Cross-sectional geometry of Pecos Pueblo femora and tibiae--a biomechanical investigation: II. sex, age, side differences. Am. J. Phys. Anthropol. 60, 383–400.

Ruff, C.B., Larsen, C.S., Hayes, W.C., 1984. Structural changes in the femur with the transition to agriculture on the Georgia coast. Am. J. Phys. Anthropol. 64, 125–36.

Ruff, C.B., Trinkaus, E., Holliday, T.W., 1997. Body mass and encephalization in Pleistocene Homo. Nature 387, 173-176.

Ruff, C.B., Holt, B., Niskanen, M., Sladek, V., Berner, M., Garofalo, E., Garvin, H.M., Hora, M., Junno, J., Schuplerova, E., Vilkama, R., Whittey, E., 2015. Gradual decline in mobility with the adoption of food production in Europe. Proc. Natl. Acad. Sci. 112, 7147 – 7152.

Ryan, T.M., Ketcham, R.A., 2002. The three-dimensional structure of trabecular bone in the femoral head of strepsirrhine primates. J. Hum. Evol. 43, 1–26.

Ryan, T.M., Krovitz, G.E., 2006. Trabecular bone ontogeny in the human proximal femur. J. Hum. Evol. 51, 591–602.

Ryan, T.M., Shaw, C.N., 2012. Unique suites of trabecular bone features characterize locomotor behavior in human and non-human anthropoid primates. PLoS One 7, e41037.

Ryan, T.M., Shaw, C.N., 2013. Trabecular bone microstructure scales allometrically in the primate humerus and femur. Proc. Biol. Sci. 280, 20130172.

Ryan, T.M., Shaw, C.N., 2015. Gracility of the modern Homo sapiens skeleton is the result of decreased biomechanical loading. Proc. Natl. Acad. Sci. 112, 372–377.

Salmon, P.L., Ohlsson, C., Shefelbine, S.J., Doube, M., 2015. Structure model index does not measure rods and plates in trabecular bone. Front. Endocrinol. 6, 1–10.

Saparin, P., Scherf, H., Hublin, J.-J., Fratzl, P., Weinkamer, R., 2011. Structural adaptation of trabecular bone revealed by position resolved analysis of proximal femora of different primates. Anat. Rec. (Hoboken). 294, 55–67.

Scherf, H., Harvati, K., Hublin, J.-J., 2013. A comparison of proximal humeral cancellous bone of great apes and humans. J. Hum. Evol. 65, 29–38.

Scherf, H., Wahl, J., Hublin, J.J., Harvati, K., 2016. Patterns of activity adaptation in humeral trabecular bone in Neolithic humans and present-day people. Am. J. Phys. Anthropol. 159, 106–115.

Shaw, C.N., Stock, J.T., 2009a. Intensity, repetitiveness, and directionality of habitual adolescent mobility patterns influence the tibial diaphysis morphology of athletes. Am. J. Phys. Anthropol. 140, 149–59.

Shaw, C.N., Stock, J.T., 2009b. Habitual throwing and swimming correspond with upper limb diaphyseal strength and shape in modern human athletes. Am. J. Phys. Anthropol. 140, 160–72.

Shaw, C.N., Ryan, T.M., 2012. Does skeletal anatomy reflect adaptation to locomotor patterns? Cortical and trabecular architecture in human and nonhuman anthropoids. Am. J. Phys.

Anthropol. 147, 187–200.

Shaw, C.N., Stock, J.T., 2013. Extreme mobility in the Late Pleistocene? Comparing limb biomechanics among fossil Homo, varsity athletes and Holocene foragers. J. Hum. Evol. 64, 242–249.

Shaw, C.N., Stock, J.T., Davies, T.G., Ryan, T.M., 2014. Does the distribution and variation in cortical bone along lower limb diaphyses reflect selection for locomotor economy? In: Carlson, K. and Marchi, D. (eds). In: Reconstructing Mobility. Springer, New York, pp. 49–66.

Sheikzadeh, A., Kendall, O., Frankel, V., 2012. Biomechanics of the hip. In: Nording, M., Frankel, V.H. (eds.), Basic Biomechanics of the Musculoskeletal System. Wolters Kluwer, Baltimore, pp. 206–223.

Skedros, J.G., Sybrowsky, C.L., Parry, T.R., Bloebaum, R.D., 2003. Regional differences in cortical bone organization and microdamage prevalence in Rocky Mountain mule deer. Anat. Rec. A. Discov. Mol. Cell. Evol. Biol. 274, 837–850.

Skinner, M.M., Stephens, N.B., Tsegai, Z.J., Foote, A.C., Nguyen, N.H., Gross, T., Pahr, D.H., Hublin, J., Kivell, T.L., 2015. Human-like hand use in Australopithecus africanus. Science 347, 395–400.

Squire, M., Brazin, A., Keng, Y., Judex, S., 2008. Baseline bone morphometry and cellular activity modulate the degree of bone loss in the appendicular skeleton during disuse. Bone. 42, 341–349.

Stansfield, B.W., Nicol, A.C., Paul, J.P., Kelly, I.G., Graichen, F., Bergmann, G., 2003. Direct comparison of calculated hip joint contact forces with those measured using instrumented implants. An evaluation of a three-dimensional mathematical model of the lower limb. J. Biomech. 36, 929–936.

Starling, A.P., Stock, J.T., 2007. Dental indicators of health and stress in early Egyptian and Nubian agriculturalists : a difficult transition and gradual recovery. Am. J. Phys. Anthropol. 134, 520–528.

Stauffer, R.N., Chao, E.Y.S., Brewster, R.L., 1977. Force and mtion analysis of the normal, diseased, and prosthetic ankle joints. Clin. Orthop. 127, 189–196.

Stock, J., Pfeiffer, S., 2001. Linking structural variability in long bone diaphyses to habitual behaviors: foragers from the southern African Later Stone Age and the Andaman Islands. Am. J. Phys. Anthropol. 115, 337–48.

Stock, J.T., 2006. Hunter-gatherer postcranial robusticity relative to patterns of mobility, climatic adaptation, and selection for tissue economy. Am. J. Phys. Anthropol. 131, 194–204.

Stock, J.T., O'Neill, M.C., Ruff, C.B., Zabecki, M., Shackelford, L.L., Rose, J.C., 2011. Body size, skeletal biomechanics, mobility and habitual activity from the late Palaeolithic to the Mid-Dynastic Nile Valley. In: Stock, J.T., Pinhasi, R. (eds.) The Bioarchaeology of the Transition to Agriculture. Wiley - Blackwell, Chichester, pp. 347–367.

Su, A., Wallace, I.J., Nakatsukasa, M., 2013. Trabecular bone anisotropy and orientation in an Early Pleistocene hominin talus from East Turkana, Kenya. J. Hum. Evol. 64, 667–77.

Sugiyama, T., Price, J.S., Lanyon, L.E., 2010. Functional adaptation to mechanical loading in both cortical and cancellous bone is controlled locally and is confined to the loaded bones. Bone 46, 314–321.

Taylor, W.R., Heller, M.O., Bergmann, G., Duda, G.N., 2004. Tibio-femoral loading during human gait and stair climbing. J. Orthop. Res. 22, 625–632.

Thompson, A.H., Chaix, L., Richards, M.P., 2008. Stable isotopes and diet at ancient Kerma, upper Nubia (Sudan). J. Archaeol. Sci. 35, 376–387.

Trinkaus, E., Ruff, C.B., 2012. Femoral and Tibial Diaphyseal Cross-Sectional Geometry in Pleistocene. PaleoAnthropology. 13–62.

Trinkaus, E., Churchill, S.E., Ruff, C.B., 1994. Postcranial robusticity in Homo. II: humeral bilateral asymmetry and bone plasticity. Am. J. Phys. Anthropol. 93, 1–34.

Turner, C.H., Hsieh, Y., Muller, R., Bouxsein, M.L., Baylink, D.J., Rosen, C.J., Grynpas, M.D.,

Donahue, L.R.A.E., Beamer, W.G., 2000. Genetic regulation of cortical and trabecular bone strength and microstructure in inbred strains of mice. J. Bone Miner. Res. 15, 1126–1131.

Ulrich, D., van Rietbergen, B., Laib, A., Rüegsegger, P., 1999. The ability of three-dimensional structural indices to reflect mechanical aspects of trabecular bone. Bone 25, 55–60.

Vaughan, L.C., Mason, B.J.E., 1975. A clinico-pathological study of racing accidents in horses. A report of a study on equine fatal accidents on racecourses. Bartholomew Press, Dorking.

Wallace, I.J., Tommasini, S.M., Judex, S., Garland, T., Demes, B., 2012. Genetic variations and physical activity as determinants of limb bone morphology: an experimental approach using a mouse model. Am. J. Phys. Anthropol. 148, 24–35.

Wallace, I.J., Kwaczala, A.T., Judex, S., Demes, B., Carlson, K.J., 2013. Physical activity engendering loads from diverse directions augments the growing skeleton. J. Musculoskelet. Neuronal Interact. 13, 283–8.

Ward, C. V., 2002. Interpreting the posture and locomotion of Australopithecus afarensis: Where do we stand? Am. J. Phys. Anthropol. 119, 185–215.

Will, M., Stock, J.T., 2015. Spatial and temporal variation of body size among early Homo. J. Hum. Evol. 82, 15–33.

Wolff, J., 1867. Ueber die innere Architectur der Knochen und ihre Bedeutung für die Frage vom Knochenwachsthum. Arch. für Pathol. Anat. und Physiol. und für Klin. Med. 50, 389 – 450.

Figures

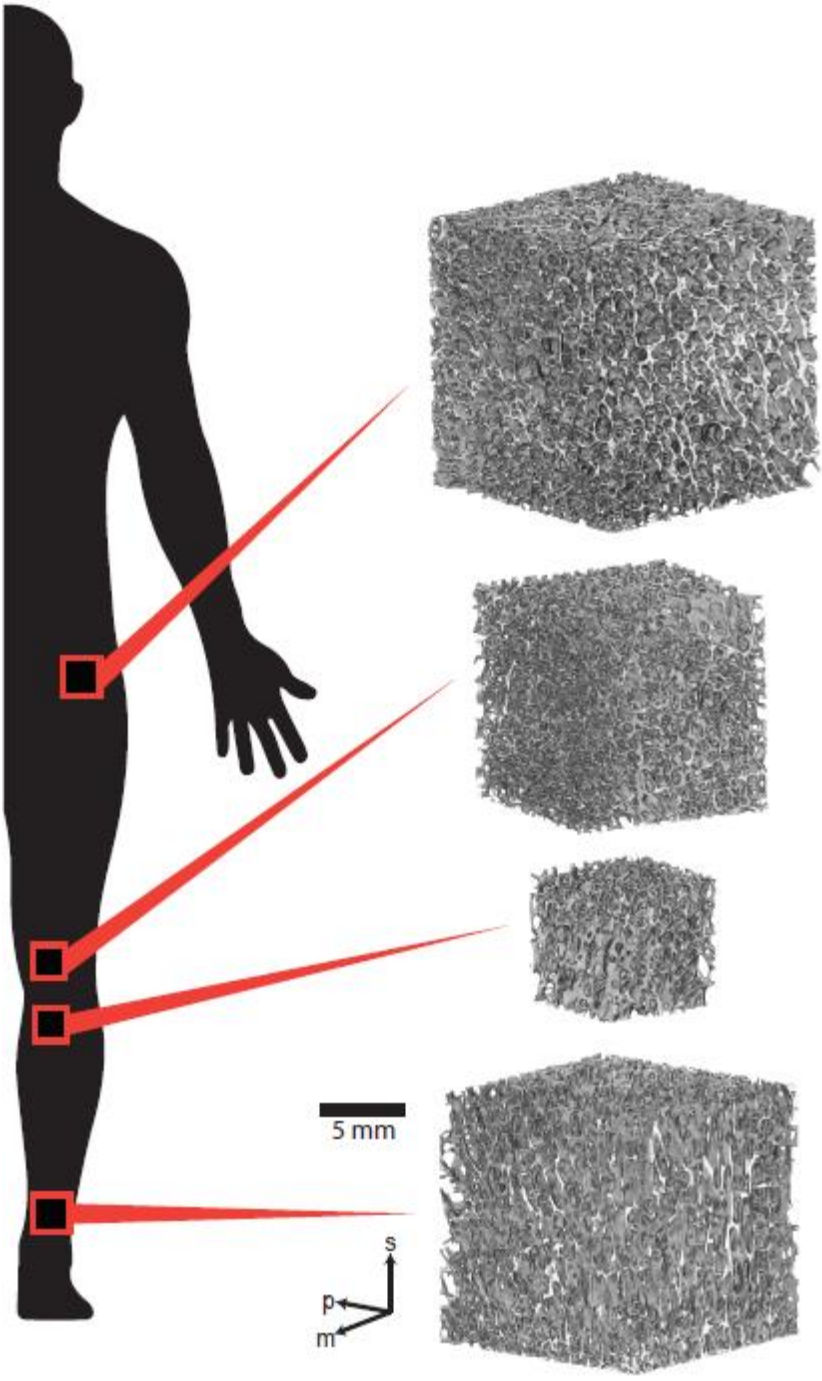

Figure 1. Cubic VOI locations and relative size differences. Black arrows denote the superior (s), posterior (p), and medial (m) axes.

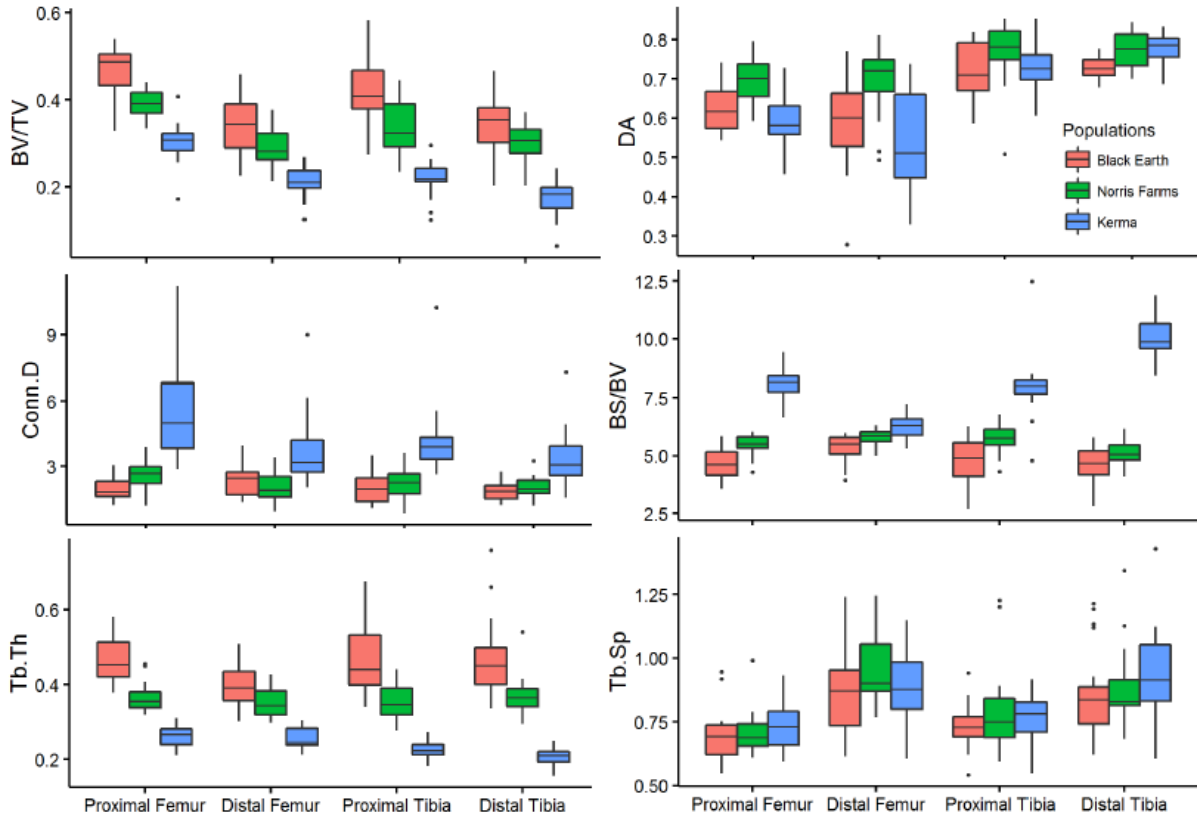

Figure 2. Boxplots of trabecular bone structural properties throughout the lower limb in individual populations. The bar indicates the median, the box contains the interquartile range, whiskers denote the minimum and maximum, and dots denote outliers. BV/TV = bone volume fraction, Tb.Th = trabecular thickness, Tb.Sp = trabecular separation, Conn.D = connectivity density, DA = degree of anisotropy, BS/BV = bone surface-area-to-volume ratio.

Tables

Table 1. Attributes of the populations included in this study

Population	**Geographic location**	**Subsistence strategy**	**Sex**		**Body mass (SD) in kg**	**Relative mobility**
			Male	Female		
Black Earth	Illinois, USA	Hunter-gatherers	11	9	63.72 (3.91) 55.19 (2.78)	High
Norris Farms	Illinois, USA	Mixed agriculture and foraging	10	10	66.36 (9.02) 60.17 (6.41)	Intermediate
Kerma	Sudan	Agriculture	13	7	66.35 (8.40) 56.74 (5.07)	Low

Table 2. Pooled sex mean (SD) of trabecular microstructural properties[a] in individual and pooled populations.

	Proximal femur	Distal femur	Proximal tibia	Distal tibia
Black Earth (*n*)	**20**	**19**	**18**	**20**
BV/TV	0.464 (0.060)	0.342 (0.065)	0.417 (0.079)	0.346 (0.070)
Tb.Th	0.464 (0.057)	0.397 (0.058)	0.467 (0.096)	0.469 (0.104)
Tb.Sp	0.696 (0.101)	0.861 (0.166)	0.732 (0.091)	0.856 (0.180)
Conn.D	1.959 (0.505)	2.337 (0.754)	1.973 (0.674)	1.854 (0.465)
DA	0.627 (0.059)	0.591 (0.121)	0.719 (0.074)	0.726 (0.027)
BS/BV	4.670 (0.630)	5.311 (0.602)	4.761 (0.950)	4.615 (0.813)
Norris Farms (*n*)	**18**	**20**	**19**	**16**
BV/TV	0.391 (0.034)	0.289 (0.048)	0.330 (0.067)	0.301 (0.051)
Tb.Th	0.363 (0.039)	0.350 (0.040)	0.353 (0.047)	0.371 (0.056)
Tb.Sp	0.708 (0.085)	0.954 (0.137)	0.792 (0.171)	0.884 (0.166)
Conn.D	2.630 (0.697)	2.021 (0.628)	2.243 (0.723)	2.040 (0.512)
DA	0.694 (0.055)	0.696 (0.088)	0.767 (0.081)	0.772 (0.045)
BS/BV	5.458 (0.465)	5.800 (0.355)	5.745 (0.621)	5.166 (0.560)
Kerma (*n*)	**20**	**18**	**18**	**20**
BV/TV	0.304 (0.048)	0.210 (0.037)	0.218 (0.042)	0.173 (0.041)
Tb.Th	0.264 (0.029)	0.254 (0.029)	0.225 (0.025)	0.207 (0.025)
Tb.Sp	0.732 (0.095)	0.885 (0.160)	0.766 (0.103)	0.934 (0.184)
Conn.D	5.616 (2.404)	3.734 (1.751)	4.177 (1.680)	3.285 (1.311)
DA	0.593 (0.068)	0.530 (0.133)	0.727 (0.064)	0.777 (0.038)
BS/BV	8.147 (0.757)	6.275 (0.561)	7.920 (1.465)	10.109 (0.925)
Pooled Data (*n*)	**58**	**57**	**55**	**56**
BV/TV	0.389 (0.081)	0.282 (0.074)	0.322 (0.103)	0.272 (0.094)
Tb.Th	0.367 (0.092)	0.335 (0.073)	0.349 (0.117)	0.347 (0.132)
Tb.Sp	0.711 (0.094)	0.901 (0.157)	0.764 (0.128)	0.892 (0.178)
Conn.D	3.325 (2.110)	2.668 (1.341)	2.788 (1.475)	2.418 (1.560)
DA	0.639 (0.073)	0.609 (0.132)	0.738 (0.075)	0.758 (0.043)
BS/BV	6.021 (1.598)	5.787 (0.639)	6.135 (1.683)	6.734 (2.664)

[a] BV/TV = bone volume fraction, Tb.Th = trabecular thickness, Tb.Sp = trabecular separation, Conn.D = connectivity density, DA = degree of anisotropy, BS/BV = bone surface-area-to-volume ratio.

Table 3. Kruskal-Wallis post hoc comparison of trabecular properties[a] throughout the lower limb between populations. *P* values adjusted for multiple comparisons, significant results are in bold.

	Black Earth versus Kerma	**Norris Farms versus Black Earth**	**Kerma versus Norris Farms**
	p (test statistic)	*p* (test statistic)	*p* (test statistic)
Proximal femur			
BV/TV	**.000 (34.0)**	**.019 (14.6)**	**.001 (19.4)**
Tb.Th	**.000 (37.7)**	**.003 (17.5)**	**.001 (20.3)**
Tb.Sp	.390 (7.1)	.853 (2.9)	.722 (4.2)
DA	.687 (6.6)	**.006 (16.5)**	**.000 (23.1)**
Conn.D	**.000 (33.5)**	**.044 (13.1)**	**.001 (20.5)**
BS/BV	**.000 (35.8)**	**.034 (13.5)**	**.000 (22.3)**
Distal femur			
BV/TV	**.000 (30.8)**	.136 (10.6)	**.001 (20.1)**
Tb.Th	**.000 (32.9)**	.253 (9.2)	**.000 (23.7)**
Tb.Sp	.929 (0.5)	.212 (2.4)	.389 (1.9)
DA	.435 (8.0)	**.035 (13.4)**	**.000 (21.3)**
Conn.D	**.006 (17.0)**	.818 (5.8)	**.000 (22.8)**
BS/BV	**.000 (25.0)**	.054 (12.6)	.062 (12.5)
Proximal tibia			
BV/TV	**.000 (31.2)**	.071 (11.9)	**.001 (19.3)**
Tb.Th	**.000 (34.5)**	**.030 (13.6)**	**.000 (20.9)**
Tb.Sp	.431 (6.6)	.663 (4.6)	.917 (2.0)
DA	.991 (0.7)	.077 (11.4)	.102 (10.8)
Conn.D	**.000 (27.6)**	1.000 (4.6)	**.000 (23.1)**
BS/BV	**.000 (31.3)**	.059 (12.3)	**.001 (19.0)**
Distal tibia			
BV/TV	**.000 (30.4)**	.491 (7.6)	**.000 (22.8)**
Tb.Th	**.000 (33.3)**	.090 (11.9)	**.000 (21.4)**
Tb.Sp	.283 (7.9)	.929 (1.9)	.521 (5.9)
DA	**.000 (20.1)**	**.005 (17.3)**	1.000 (2.8)
Conn.D	**.000 (21.8)**	1.000 (4.3)	**.004 (17.6)**
BS/BV	**.000 (31.0)**	.652 (6.8)	**.000 24.3)**

[a] BV/TV = bone volume fraction, Tb.Th = trabecular thickness, Tb.Sp = trabecular separation, Conn.D = connectivity density, DA = degree of anisotropy, BS/BV = bone surface-area-to-volume ratio.

Table 4. Kruskal-Wallis post hoc comparison of trabecular properties[a] across the limb in a pooled sample of all populations. *P* values adjusted for multiple comparisons, significant results are in bold.

	Proximal femur	**Distal femur**	**Proximal tibia**
	p (test statistic)	*p* (test statistic)	*p* (test statistic)
BV/TV			
Distal femur	**.000 (71.7)**	X	
Proximal tibia	**.001 (45.6)**	.205 (26.2)	X
Distal tibia	**.000 (76.0)**	1.000 (4.3)	.085 (30.5)
Tb.Th			
Distal femur	.483 (19.9)	X	
Proximal tibia	.922 (15.8)	.985 (4.1)	X
Distal tibia	.894 (16.9)	.991 (3.0)	1.00 (1.1)
Tb.Sp			
Distal femur	**.000 (84.2)**	X	
Proximal tibia	.168 (27.0)	**.000 (57.1)**	X
Distal tibia	**.000 (76.2)**	1.000 (7.9)	**.000 (49.2)**
Conn.D			
Distal femur	.401 (19.0)	X	
Proximal tibia	.743 (12.4)	.951 (6.6)	X
Distal tibia	**.041 (32.4)**	.698 (13.4)	.374 (20.0)
DA			
Distal femur	1.000 (0.4)	X	
Proximal tibia	**.000 (71.8)**	**.000 (71.4)**	X
Distal tibia	**.000 (86.6)**	**.000 (86.2)**	1.000 (14.8)
BS/BV			
Distal femur	.871 (9.3)	X	
Proximal tibia	.824 (10.6)	1.000 (1.3)	X
Distal tibia	.957 (6.7)	1.000 (2.6)	.998 (3.9)

[a] BV/TV = bone volume fraction, Tb.Th = trabecular thickness, Tb.Sp = trabecular separation, Conn.D = connectivity density, DA = degree of anisotropy, BS/BV = bone surface-area-to-volume ratio.

Table 5: Coefficients of variation of trabecular properties[a] from pooled sex samples throughout the lower limb.

	BV/TV	Tb.Th	Tb.Sp	SMI	Conn.D	DA	BS/BV
Proximal femur							
Black Earth	0.1299	0.1226	0.1453	0.6733	0.2579	0.0946	0.1348
Norris Farms	0.0860	0.1080	0.1199	0.1851	0.2717	0.0785	0.0855
Kerma	0.1595	0.1099	0.1304	0.1978	0.4280	0.1139	0.0929
Pooled	0.2087	0.2509	0.1318	0.4314	0.6345	0.1141	0.2654
Distal femur							
Black Earth	0.1914	0.1453	0.1928	0.2324	0.3228	0.2044	0.1133
Norris Farms	0.1674	0.1142	0.1434	0.1578	0.3106	0.1261	0.0612
Kerma	0.1769	0.1127	0.1811	0.2027	0.4688	0.2510	0.0894
Pooled	0.2637	0.2183	0.1742	0.2715	0.5028	0.2174	0.1104
Proximal tibia							
Black Earth	0.1976	0.2358	0.1322	0.3862	0.3999	0.1076	0.2515
Norris Farms	0.2030	0.1337	0.2153	0.1944	0.3224	0.1053	0.1081
Kerma	0.1794	0.1142	0.1215	0.1631	0.4150	0.0791	0.1907
Pooled	0.3203	0.3351	0.1672	0.3070	0.5290	0.1016	0.2744
Distal tibia							
Black Earth	0.2033	0.2210	0.2104	0.2257	0.2510	0.0370	0.1762
Norris Farms	0.2382	0.1206	0.1975	0.1324	0.3991	0.0485	0.0915
Kerma	0.1692	0.1514	0.1878	0.1193	0.2509	0.0587	0.1085
Pooled	0.3457	0.3800	0.1994	0.1941	0.4475	0.0572	0.3957

[a] BV/TV = bone volume fraction, Tb.Th = trabecular thickness, Tb.Sp = trabecular separation, Conn.D = connectivity density, DA = degree of anisotropy, BS/BV = bone surface-area-to-volume ratio